Research Article Adv. Mat. Lett. 2014, **5**(12), 692-698 ADVANCED MATERIALS *Letters*

www.amlett.com, www.vbripress.com/aml, DOI: 10.5185/amlett.2014.7588

Structural and hydrogen storage properties of Mg-x wt% ZrCrMn composites

Ankur Jain[1,2,3]*, Pragya Jain[1], Shivani Agarwal[1,3], Paola Gislon[3], Pier Paolo Prosini[3], I.P. Jain[1]

[1]*Centre for Non-Conventional Energy Resources, University of Rajasthan, Jaipur, India*
[2]*Institute for Advanced Materials Research, Hiroshima University, Higashi-Hiroshima 739-8530, Japan*
[3]*ENEA-IDROCOMB, C.R. Casaccia, Via Anguillarese 301, 00060 S. Maria di Galeria, Rome, Italy*

*Corresponding author. Tel: (+91) 141 2711049; E-mail: ankur.j.ankur@gmail.com

Received: 03 July 2014, Revised: 27 July 2014 and Accepted: 03 August 2014

ABSTRACT

Magnesium hydride is a promising material for hydrogen storage due to its high storage capacity i.e.7.6wt%. But its high stability i.e. high desorption temperature (~350°C) limits its practical application towards hydrogen economy. Moreover the kinetics is also too slow even at high temperatures. Composite formation with Zr based laves phase alloys, especially $ZrCr_2$ family, is an effective method to improve the hydriding properties of MgH_2. This work presents the synthesis, structural, morphological, and hydrogenation properties of Mg-x wt% ZrCrMn composites. Both phases i.e. Mg & ZrCrMn remain their presence after milling and several hydriding cycles as well. SEM results suggest the homogeneous distribution of alloy particles on Mg matrix. Pressure composition temperature (PCT) analysis shows a reduction in desorption temperature down to 250°C for these composites. TG experiments suggest a total hydrogen capacity of 5.9% and 4.35% for x =25, 50 in Mg-x wt% ZrCrMn composites respectively. The enthalpy of hydride formation is also calculated using Van't Hoff plots, which is found similar to the parent material i.e. MgH_2. A remarkable enhancement in the kinetics of hydrogen absorption / desorption is reported here by forming these composites.

Keywords: Hydrogen storage; magnesium; ball milling; kinetics; X-ray diffraction; microstructures.

Ankur Jain is working as researcher at Institute of Advanced Materials Research, Hiroshima University, Japan. He obtained his Ph.D. in 2007 from University of Rajasthan-Jaipur, India. He has been recipient of several prestigious fellowships and awards including ICTP-TRIL, Italy; JSPS PDF, Japan. He has published more than 35 research papers and several conference proceeding papers.

Pier Paolo Prosini is Senior Research Scientist at ENEA – Italian National Agency for New Technologies, Energy and Sustainable economic development, Italy. He has authored several research papers, books, patents. He is member of several Italian and International Societies. He is actively engaged with several research fields including fuel cell, batteries, and hydrogen storage material research.

I.P. Jain is Emeritus Professor at Centre for Non-Conventional Energy Resources, University of Rajasthan, Jaipur, India. He has been founder director of above mentioned Centre. He authored more than 150 research articles. He has delivered more than 50 keynote and invited talk at various meetings, conferences worldwide. He is actively engaged with several research topics such as hydrogen storage materials and applications, thin films, surface and interfaces, ion beam mixing at metal/silicon surfaces and interfaces, and amorphous semiconductors.

Introduction

Hydrogen storage is a key issue to establish hydrogen economy efficiently. During last few decades intensive research efforts have been carried out in order to get suitable storage material. Although several new complex hydrides **[1]** have been proposed as a result of these efforts, metal hydrides are still considered as important materials for hydrogen storage **[2]**. Magnesium and its derived alloys are considered the most attractive contender **[2, 3]** due to their unique characteristics towards hydrogen storage such as high theoretical value of H content i.e. 7.6 wt% for MgH_2, good reversibility, low cost and abundant availability. On the other side, the drawbacks associated with MgH_2 are high working temperature (>300^{o}C due to high enthalpy of formation), poor kinetics and hard activation process. These drawbacks create hurdles for the hydrogen community to use MgH_2 as practical storage media. Tremendous efforts have been adopted to improve the hydrogen storage properties of MgH_2, namely nano-structuring **[4, 5]**, alloying **[6-8]** and addition of catalytic materials **[9-11]**. Nano-structuring achieved through the communication of Mg / MgH_2 particles with high energy ball milling is considered as a successful tool in enhancing bulk properties of magnesium due to several defects creation and the reduction in grain size. However, the use of high energy ball milling is far away to achieve the required size (<5 nm) that is necessary to improve the thermodynamics **[12, 13]**. The second approach of alloying Mg with other elements, thus forming alloys such as Mg_2Ni **[6]**, Mg_2Co **[7]**, Mg-La **[8]** etc succeeded in reducing the formation enthalpy, but the addition of other elements reduce the total capacity as well. The third approach, using catalysts such as Ti, Zr, Fe, Ni **[9]**, Nb_2O_5 **[10]**, Cr_2O_3 **[11]** has shown great potential to enhance the reaction kinetics by decreasing the activation energy necessary to dissociate hydrogen. Since the hydrogenation performance of a Mg – M composite material is directly influenced by the interaction of different components of the system with hydrogen, the kinetic performance of Mg can be improved by the addition of some low temperature hydrides having good kinetic behavior towards hydrogen absorption / desorption. Thus apart from the transition metals or their oxides, hydrogen storage species such as $LaNi_5$ **[14, 15]**, FeTi **[16, 17]**, $MmNi_5$ **[18]**, Zr based AB_2 alloy **[19-24]** have been attempted and shown good results to improve the hydrogen storage characteristics of Mg by composite formation. Recently Dehouche et al **[21]** and Pighin et al **[22]** achieved enhanced kinetics of MgH_2 by the addition of Zr-Ni alloys. They found Zr_8Ni_{21} as a better additive in comparison to other stoichiometries of Zr-Ni alloys. $ZrMn_2$ is another good material belonging to this family which has made Mg capable to absorb hydrogen at room temperature in a report by Makihara et al **[23]**. The authors explained this improvement in terms of elastic interaction between MgH_2 and $ZrMn_2H_x$ through their interface boundary. Recent attention has been paid to the $ZrCr_2$ based alloys as a catalytic / composite alloy for Mg / MgH_2 **[24-30]**. In a study on $ZrCr_{1.8}Cu_{0.3}$ / Mg composite material by Orimo et al **[24]**, it is shown that the nucleation sites for the MgH_2 phase is provided by the interface boundaries of Mg_2Cu / Mg eutectic which is formed during a heat treatment of the composite material. These interface boundaries act as diffusion path for hydrogen atoms from $ZrCr_{1.8}Cu_{0.3}$ phase to Mg phase. Agarwal et al **[28]** achieved reduction in desorption temperature down to 250°C for Mg-ZrCrNi composite with a reversible capacity of 5.8 wt%. Further destabilization could be possible by preparing Mg composite with ZrCrCu in place of ZrCrNi **[29, 30]**. However, the hydrogen absorption / desorption kinetics was found better for ZrCrNi composite due to the presence of Ni - a highly catalytic element for hydrogenation **[29]**. In our recent work **[31]** we have shown the simultaneous catalytic and hydriding behavior of alloy phase in Mg-ZrCrFe composite at high and low temperature respectively, thus resulting in a total capacity of 4.5 wt%, which is higher than any other similar reported work. Since it is clear from the recent literature **[28-31]** that the third element M in ZrCrM alloy has varying effect on hydrogen storage properties of Mg-ZrCrM composites, thus it is important to explore the effect of different elements in order to get better understanding of these composites. We have already explored all other transition metals as mentioned above **[28-31]**, Mn out of this group is still to be explored. Thus present work is focused to study ZrCrMn alloy as a counter part of composite material with Mg. Herein, we present the structural, morphological, kinetics and sorption isotherms of Mg-x wt% ZrCrMn composites. The results obtained are compared with the published data on other ZrCrM systems.

Experimental

Sample preparation

ZrCrMn alloy is prepared by arc melting of constituent elements [Zr (99.8%), Cr (99.9%), Mn (99.9%); all from Sigma Aldrich] in a stoichiometric ratio under Ar flow. The alloy button is remelted four times by turning it upside down after each solidification to ensure homogeneity. Ti sponge was used as oxygen getter to avoid any oxidation, even due to the impurity of carrier gas. The alloy button is crushed into powder form and this powder is used to prepare composites with Mg. Mg and ZrCrMn alloy powder are milled together under 5 bar Ar pressure in a Spex 8000 mixer miller for 5 hours with a sequence of 30 min work and 5 min rest to avoid over-heating. The ball to powder ratio is kept 10:1. The handling of samples is done in an Ar filled glove box.

Characterization and hydrogen storage measurements

A Miniflex Rigaku diffractometer with CuKα radiation is used to characterize the present phases in the composites. Scanning Electron Microscopy (JEOL JSM 5510 LV) is employed to see the powder morphology of all the samples. In addition, elemental mapping is performed using Energy Dispersive X-ray (EDX) analysis with an IXRF EDS-2000 system equipped with SEM. The absorption / desorption P-C isotherms of these composites are recorded using a specifically designed PCT apparatus from DeltaE, University of Calabria, Italy (www.deltae.it). The absorption/desorption kinetics measurements are also performed on the same system at constant pressures of 10 bar and 0.1 bar respectively for temperatures 250 – 300°C. Thermal gravimetric analysis is made on a TA Instruments SDT Q 600 supported by a computer running Thermal Advantage software kit for data acquisition. The temperature sensor is calibrated using the nickel Curie point as a reference. The mass is calibrated using ceramic standards provided with the instrument. A high purity aluminium oxide pan is used as the reference material and to keep the sample. Thermal scan is performed from ambient temperature to 400°C at constant heating rate of $5^{o}C\ min^{-1}$ under a high purity Ar flow with 100ml/min flow rate.

Results and discussion

The XRD pattern of powdered ZrCrMn alloy is shown in **Fig. 1** (**a**). The alloy is crystallized in hexagonal C14 type structure as that of its parent alloy $ZrCr_2$. The calculated lattice parameters of the alloy are a = 5.035 Å and c = 8.29 Å, which is in good agreement with previous report **[32]**. **Fig. 1** (**b** and **c**) show the XRD patterns of 5 h milled Mg – x wt% ZrCrMn (x = 25, 50) composites. Comparison of **Fig. 1** (**a** and **b**) reveals a decrease in the peak intensities corresponding to the ZrCrMn phase and a significant broadening in these. This behavior is frequently observed in literature, where crystalline $ZrCr_2$ based materials turned into a mixture of amorphous and nano-crystalline structures **[33]**. However, the peak intensities corresponding to

ZrCrMn in **Fig. 1**(**c**) is slightly increased with respect to **Fig. 1**(**b**), while the Mg peak intensities decreased. This must be due to the variation in fraction ratio of Mg and alloy phase. It is also noteworthy that no phase other than Mg and ZrCrMn is found visible in the pattern which consequently suggests no reaction between the elements of ZrCrMn and Mg. This is in line with the existing phase diagrams of Mg-Zr, Mg-Cr and Mg-Mn **[34]**, where no solubility for each pair is reported.

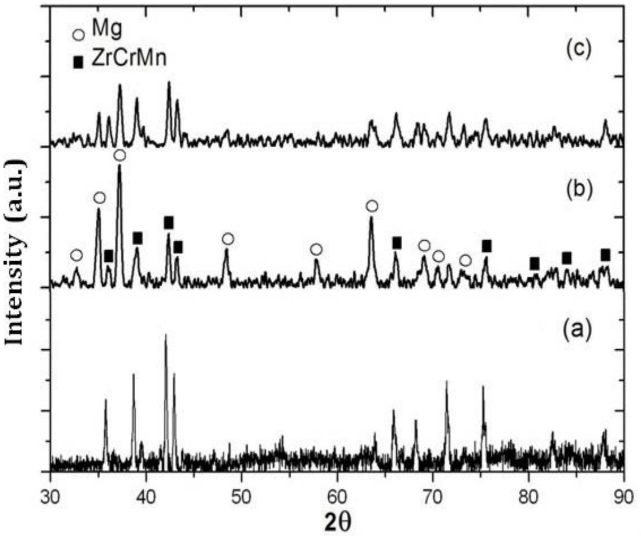

Fig. 1. XRD pattern of (**a**) ZrCrMn alloy and 5 hr milled (**b**) Mg – 25 wt% ZrCrMn and (**c**) Mg – 50 wt% ZrCrMn composites.

Fig. 2 illustrates the microstructures of Mg-x wt% ZrCrMn composites. Since magnesium is very ductile in nature, so very difficult to be grinded in to powder form. On the contrary $ZrCr_2$ based alloys are generally brittle, thus helpful to reduce the particle size of Mg, when milled together. However, Mg-25% ZrCrMn composite still shows flake type structure – a well-known micro-structural characteristic of magnesium. The increased amount of ZrCrMn content reduces the particle size and enhances the brittleness of the composite. The distribution of alloy particles on Mg matrix is confirmed using EDX Micrographs with a higher magnification are chosen for these purposes, which are shown in the upper part of **Fig. 3**; the corresponding elemental mapping using EDX is shown downwards in the same figure. It is clear from the images that the alloy particles are homogeneously distributed in the Mg matrix. The increased intensity of Zr, Cr and Mn corresponds to the increasing fraction of alloy phase in Mg – 50 wt% ZrCrMn composite.

Fig. 4 shows XRD pattern of both composites after 1 hydrogenation cycle. Hydrogenation could not promote any reaction between both counterparts except their conversion to their respective hydrides. Since Zr based alloys don't change their structure upon hydrogenation except an enlargement in crystal lattice **[35]**; the formation of the alloy hydride phase was confirmed by the shifting of alloy peaks towards left, which is indication of lattice expansion. In addition to MgH_2 and ZrCrMn-H, some peaks corresponding to Mg also exist in the pattern which suggest the un-reacted fraction of Mg and suggest the need of activation cycles.

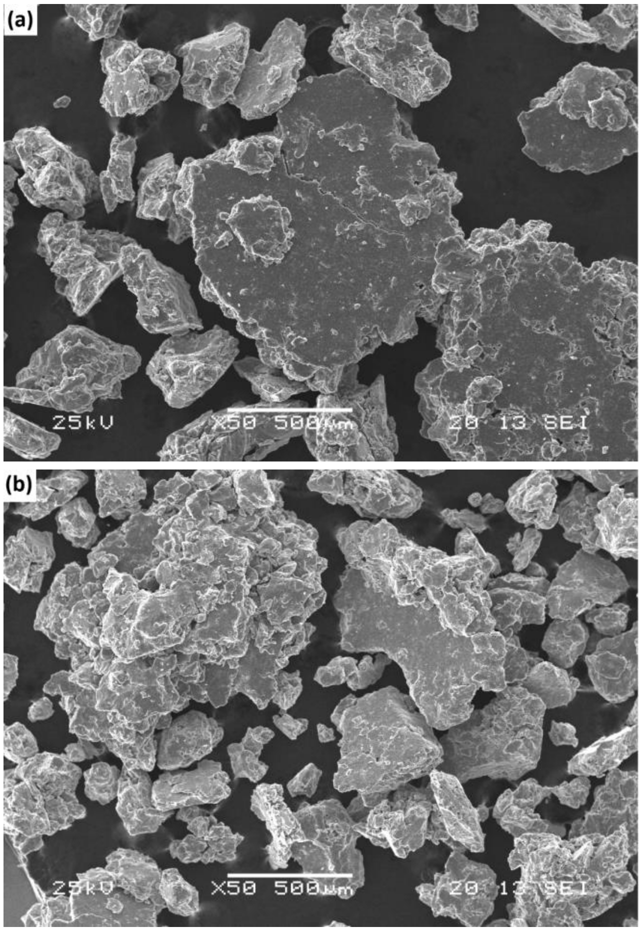

Fig. 2. SEM images showing flake structure in 5 hr milled (**a**) Mg – 25 wt% ZrCrMn and (**b**) Mg – 50 wt% ZrCrMn composites.

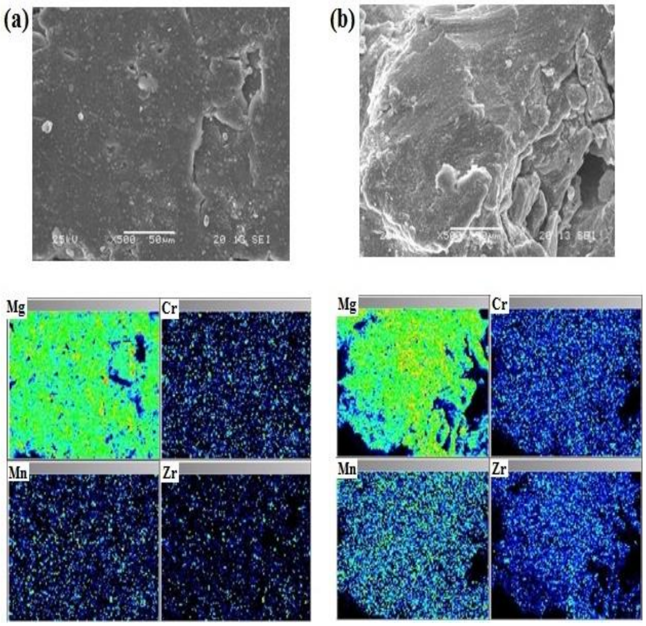

Fig. 3. SEM images & their corresponding elemental mapping showing particle morphology and alloy particle distribution of 5 hr milled (**a**) Mg – 25 wt% ZrCrMn and (**b**) Mg – 50 wt% ZrCrMn composites.

This result is supported by PCT experiments (not shown here), where the total hydrogen capacity is found to be less than the expected theoretical value.

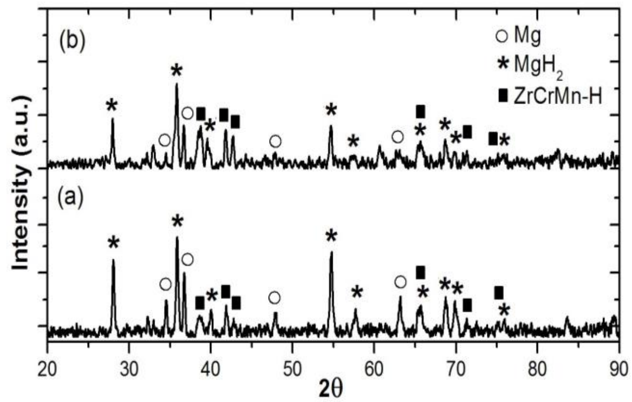

Fig. 4. XRD pattern of (**a**) Mg – 25 wt% ZrCrMn and (**b**) Mg - 50wt % ZrCrMn composites after one hydriding cycle.

Fig. 5 shows the PC isotherms of Mg-x wt% ZrCrMn composites for 3 temperatures i.e. 250, 275 and 300 °C. Since the activation cycles were found necessary in the previous works on other composites **[28-31]**, before the real measurement, some absorption/desorption cycles were performed until the stabilized results were achieved.

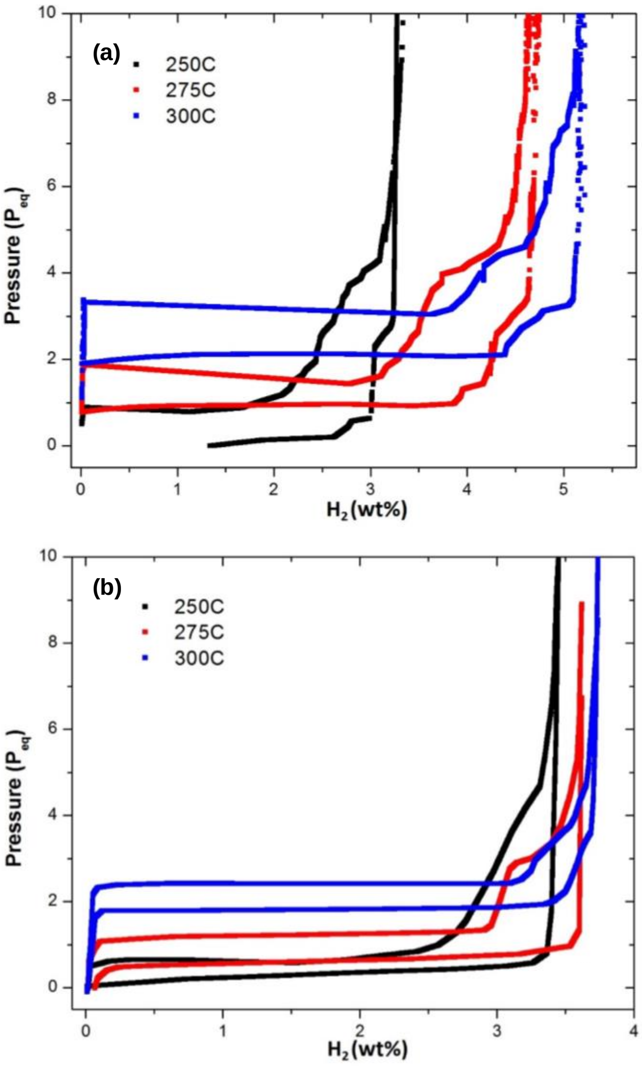

Fig. 5. P-C-T isotherms of Mg – x wt% ZrCrMn composites (**a**) x=25wt%, (**b**) x=50wt%.

The effect of alloy content in the composite is significant enough to show the lowering of the required desorption temperature in comparison to pure Mg, as for the later no complete desorption is achieved at 300°C. The composite with 25 wt% ZrCrMn shows clear plateau even at 275°C. Moreover, it desorbs half of its total hydrogen content at 250°C. This is further improved for Mg-50wt% ZrCrMn composite which desorbs all of its hydrogen content at 250^{o}C. However, the total capacity is decreased with increasing content of ZrCrMn due to its higher weight. The total maximum capacity in Mg-x wt% ZrCrMn composites is found to be 5.51 and 3.73 wt% at 300^{o}C for x = 25 and 50 respectively. These values are equal to the theoretical value of MgH$_2$ counterpart; this means ZrCrMn alloy remains silent towards the reaction with hydrogen. This is because of the separate PCT windows of Mg and ZrCrMn alloy as discussed in our recent work for Mg-50 wt% ZrCrFe composite **[31]**, where the alloy fraction of composite reacts with hydrogen in the temperature range of RT – 100°C. Thus the above values of hydrogen capacity are not real effective values. To obtain the real values we performed TG measurements on fully hydrogenated samples.

To hydrogenate the samples, the composites (same composites after PCT experiment) were exposed to 10 bar of hydrogen at 300°C in a closed reactor for 2 hours and then cool down slowly to room temperature in 6 hrs. This assures a complete hydrogen absorption by both counterparts of composite i.e. Mg and the alloy phase. Thus prepared samples were employed to TG experiment at a scan rate 10°C / min. Before making TG experiment the composites were employed to XRD to confirm its hydrogenated state and the results are shown in **Fig. 6**. No traces of Mg are found in XRD pattern in contrast to **Fig. 4**. Thus, even after several hydrogenation cycles, no reaction takes place except the conversion of Mg to MgH$_2$ and the alloy phase to its corresponding hydride phase.

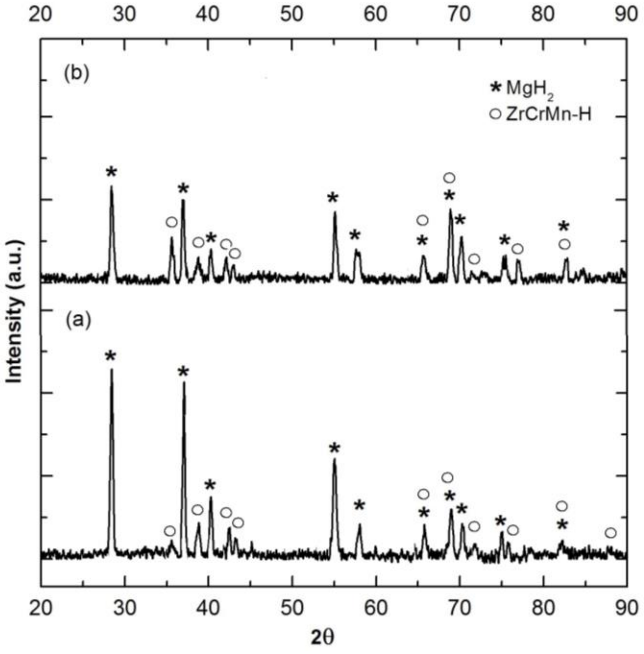

Fig. 6. XRD pattern of (**a**) Mg – 25 wt% ZrCrMn and (**b**) Mg – 50 wt% ZrCrMn composites after several hydriding cycles.

The TG spectra of Mg–x wt% ZrCrMn composites are shown in **Fig. 7**. It is noted that the hydrogen desorption starts for both the composites at 90 °C which continues until 120°C, which corresponds to the decomposition of the alloys hydride phase with a weight loss of 0.3 and 0.6 wt% for Mg-25% ZrCrMn and Mg-50% ZrCrMn composites respectively. Further increase in temperature up to 400°C increases the weight loss up to 5.9 wt% and 4.35 wt% for x = 25 and 50 in Mg-x wt% ZrCrMn composite respectively. Thus the total effective capacities for both composites are found larger than the values observed by PCT measurement. These values are very close to the theoretical value of 6.02 wt% for Mg-25% ZrCrMn and 4.44 wt% for Mg-50% ZrCrMn composite, while the hydrogenation for both counterparts is taken into account.

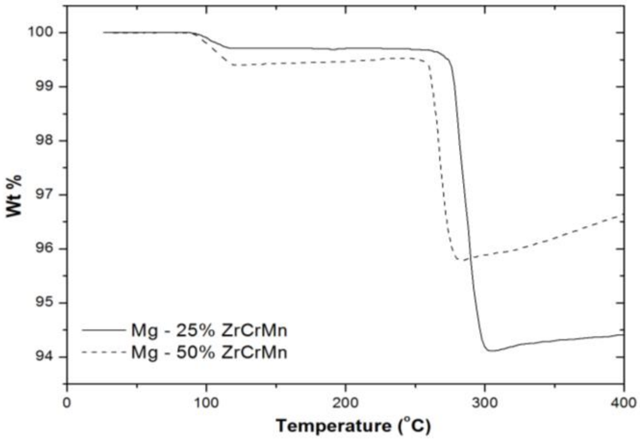

Fig. 7. TG Profile of hydrogen evolution from Mg – x wt% ZrCrMn composites.

The enthalpy (ΔH) and entropy (ΔS) of hydride formation were calculated using Van't Hoff plot of lnP vs 1/T as illustrated in **Fig. 8**. The enthalpy values of the hydrogenation process for Mg-x wt% ZrCrMn composites are found to be -70.38 and -64.30 kJ mol^{-1} for x = 25 and 50 respectively. These values are almost same as that of pure Mg **[36]**. The small variation in enthalpy values could be correlated to the defects created into the material during the ball milling. The entropy value for Mg-25% ZrCrMn is calculated as 132.78 JK^{-1}mol^{-1}, which is nearly equal to the standard entropy of hydrogen; the value of entropy is decreased to 119.37 JK^{-1}mol^{-1} for the composite having 50% ZrCrMn. This could be due to the more defects induced by the higher amount of alloy phase. In our opinion the observed complete hydrogen desorption at 250°C by Mg-50% ZrCrMn composite is not actually thermodynamic destabilization, it is rather associated with the kinetic aspect of hydrogen desorption.

The hydrogen absorption / desorption kinetics of Mg – x wt% ZrCrMn composites are shown in **Fig. 9** and **Fig. 10**. The composite with 25% ZrCrMn absorbs its total capacity in less than 20 min, while it takes only 15 min to desorb all the hydrogen at 300°C. The absorption / desorption rates are found satisfactory even at lower temperatures i.e. 250°C and 275°C. However, sample could not desorb its total capacity at 250^{o}C and half of the hydrogen capacity remains captured in the sample even after 60 min. The kinetics is further improved with increasing ZrCrMn fraction in the composite and sample desorbs more than 90% of total hydrogen content at 250°C within 60 min. This clearly shows the importance of alloy phase presence. Since the dissociation energy required by hydrogen molecule is much lower for ZrCrMn than Mg, the alloy phase works as host surface to dissociate H_2 molecule and provides diffusion path through the grain boundaries of Mg-ZrCrMn interface. Due to the presence of these diffusion channels hydrogen penetrates deeper, thus improving the overall kinetics of hydrogen absorption/desorption.

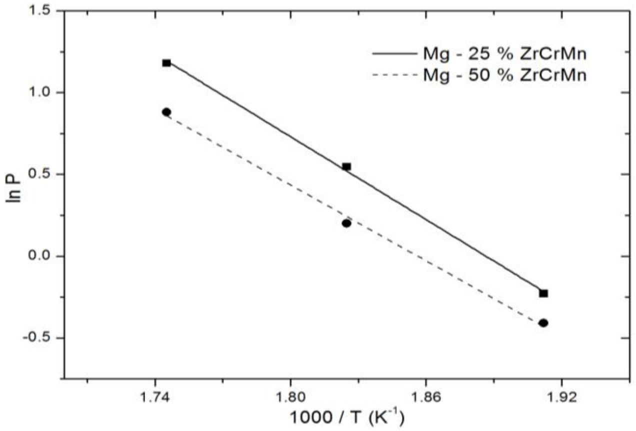

Fig. 8. Van't Hoff Plot for Mg – x wt% ZrCrMn composites.

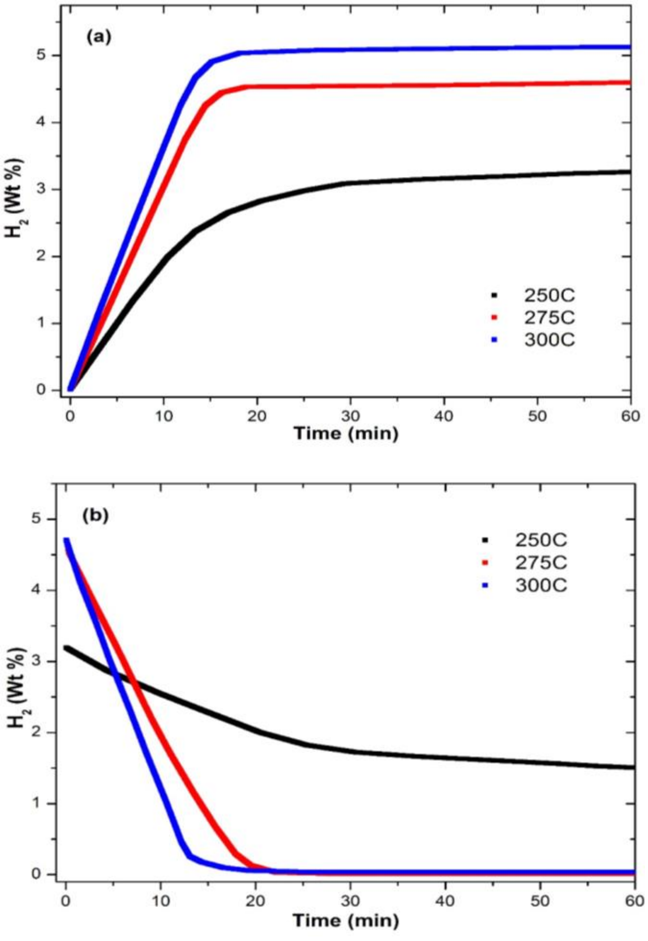

Fig. 9. (**a**) Absorption (**b**) desorption kinetics for Mg – 25 wt% ZrCrMn composite.

On comparing the kinetic behavior published in literature **[37]** it is observable that kinetics of these composites is much faster than pure Mg, but slower than MgH_2-ZrCrNi composites as reported by Agarwal et al in an earlier work **[28]**. The difference in the kinetic behaviors of composites with ZrCrMn, ZrCrCu **[29]**, ZrCrFe **[31]** is not found much significant. As discussed earlier the alloy particles behave as host surface for the dissociation of hydrogen molecule, the nature of these must be directly responsible for the variation in kinetic behavior. Since ZrCrNi is the most active material towards the interaction with hydrogen among the other materials of $ZrCr_2$ family **[38]**, this gives much better kinetic improvement than other ZrCrM alloys as composite material.

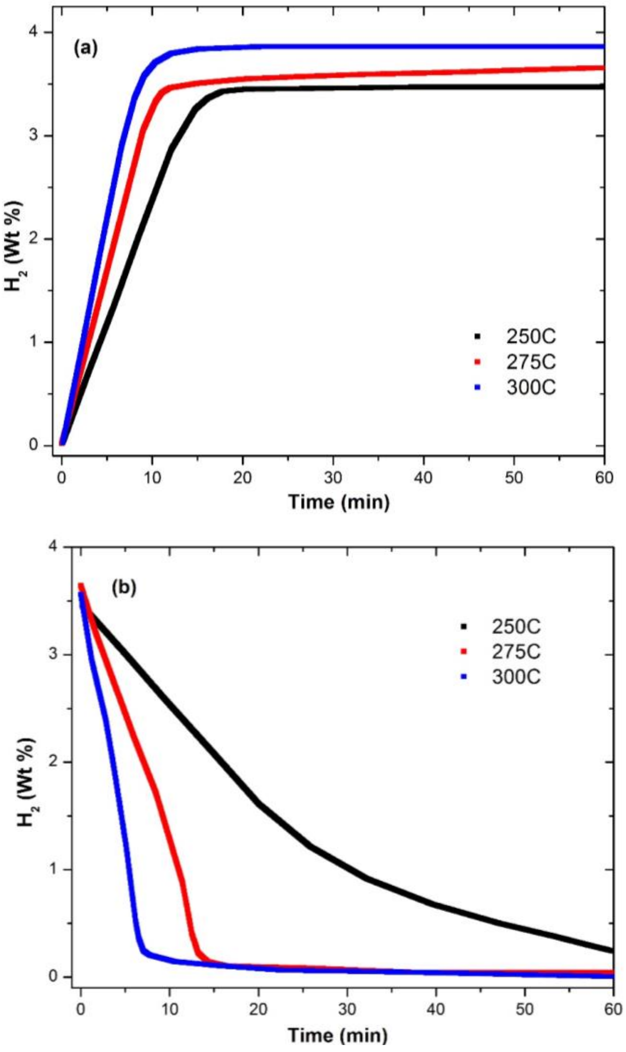

Fig. 10. (**a**) Absorption (**b**) desorption kinetics for Mg – 50 wt% ZrCrMn composite.

Conclusion

The performance of Mg – x wt% ZrCrMn alloy composites as hydrogen storage materials have been studied. ZrCrMn alloy was prepared by arc melting followed by ball milling of Mg and ZrCrMn alloy for 5 hours for composite preparation. ZrCrMn alloy crystallizes in C14 hexagonal structure and both phases i.e. Mg and ZrCrMn keep their identity in composite with no other additional phase formation. Even after several hydrogenation cycles no phase formation was observed between Mg and the alloy components; both phases converted to their respective hydride phases only. Micro-structural studies confirmed the composite nature of alloy particles showing Mg matrix decorated with a uniform distribution of alloy particles. The maximum storage capacity is found to be 5.9 and 4.35 wt% at 300°C for x = 25 and 50 respectively in Mg-x wt% ZrCrMn composite. ZrCrMn alloy shows the simultaneous behavior of hydrogen absorbing species and catalyst in a single hydrogenation cycles, but in different temperature windows. Mg-50% ZrCrMn composite succeeded in desorbing 90% of its total hydrogen content at 250°C in about 60 min.

Acknowledgements
Authors gratefully acknowledge financial support from Department of Science & Technology, New Delhi, India under FAST Track Scheme and ICTP, Trieste, Italy under TRIL program. We are thankful to Mr. Amedeo Masci, ENEA-Casaccia, Rome for making SEM images for this work.

Reference

1. Jain, I.P.; Jain, P.; Jain, A.; *J. Alloys Compd.* **2010**, *503*, 303.
DOI: 10.1016/j.jallcom.2010.04.250
2. Sakintuna, B.; Weinberger, B.; Lamari-Darkrim, F.; Hirscher, M.; Dogan, B.; *Int. J. Hydrogen Energy* **2007,** *32*, 1121.
DOI: 10.1016/j.ijhydene.2006.11.022
3. Jain, I.P.; Lal, C.; Jain, A.; *Int. J. Hydrogen Energy* **2010,** *35*, 5133.
DOI: 10.1016/j.ijhydene.2009.08.088
4. Zaluska, A.; Zaluski, L.; Ström–Olsen, J. O.; *J. Alloys Compd.* **1999,** *288*, 217.
DOI: 10.1016/S0925-8388(99)00073-0
5. Huot, J.; Liang, G.; Boily, S.; Van Neste, A.; Schulz, R.; *J. Alloys Compd.* **1999,** *293-295*, 495.
DOI: 10.1016/S0925-8388(99)00474-0
6. Gennari, F.C.; Esquivel, M.R.; *J. Alloys Compd.***2008,** *459*, 425.
DOI: 10.1016/j.jallcom.2007.04.283
7. Fernández, G.; Meyer, G.O.; Gennari, F.C.; *J. Alloys Compd.* **2008,** *464*, 111.
DOI: 10.1016/j.jallcom.2007.09.102
8. Yajima, S.; Kayano, H.; Toma, H.; *J. Less-Common Met.* **1977,** *55*, 139.
DOI: 10.1016/0022-5088(77)90272-7
9. Pozzo, M.; Alfè, D.; *Int. J. Hydrogen Energy* **2009,** *34*, 1922.
DOI: 10.1016/j.ijhydene.2008.11.109
10. Friedrichs, O.; Klassen, T.; Sánchez-López, J.C.; Bormann, R.; Fernández, A.; *Scr. Mater.* **2006**, *54*, 1293.
DOI: 10.1016/j.scriptamat.2005.12.011
11. Song, M.Y.; Bobet, J.-L.; Darriet, B.; *J. Alloys Compd.* **2002,** *340*, 256.
DOI: 10.1016/S0925-8388(02)00019-1
12. Wagemans, R. W. P.; Lenthe, J. H. van; Jongh, P.E. de; Dillen, A.J. van; Jong, K.P.; *J. Am. Chem. Soc.* **2005**, *127*, 16675.
DOI: 10.1021/ja054569h
13. Aguey-Zinsou, K.-F.; Ares-Fernández, J.-R.; *Chem. Mater.* **2008,** *20*, 376.
DOI: 10.1021/cm702897f
14. Gu, H.; Zhu, Y.; Li, L.; *Int. J. Hydrogen Energy* **2009,** *34*, 1405.
DOI: 10.1016/j.ijhydene.2008.11.078
15. Nowak M.; Jurczyk, M.; *Phys. Status Solidi A* **2010**, *207*, 1144.
DOI: 10.1002/pssa.200983391
16. Zaranski, Z.; Czujko, T.; *J. Alloys Compd.***2011,** *509*, S608.
DOI: 10.1016/j.jallcom.2010.10.063
17. Vijay, R.; Sundaresan, R.; Maiya, M.P.; Murthy, S. S.; Fu, Y.; Klein, H.P.; Groll, M.; *J. Alloys Compd.* **2004**, *384*, 283.
DOI: 10.1016/S0925-8388(02)00019-1
18. Vijay, R.; Sundaresan, R.; Maiya, M.P.; Murthy, S.S.; *Int. J. Hydrogen Energy* **2007,** *32*, 2390.
DOI: 10.1016/j.ijhydene.2006.11.011
19. Kandavel M.; Ramaprabhu, S.; *J. Phys.: Condens. Matter* **2006,** *18*, 11275.
DOI: 10.1088/0953-8984/18/49/019

20. Kandavel, M.; Ramaprabhu, S.; *J. Alloys Compd.* **2007,** *438*, 285. **DOI:** 10.1016/j.jallcom.2006.08.031
21. Dehouche, Z.; Peretti, H.A.; Hamoudi, S.; Yoo, Y.; Belkacemi, K.; *J. Alloys Compd.* **2008,** *455*, 432. **DOI:** 10.1016/j.jallcom.2007.01.138
22. Pighin, S.A.; Capurso, G.; Russo, S.L.; Peretti, H.A.; *J. Alloys Compd.* **2012,** *530*, 111. **DOI:** 10.1016/j.jallcom.2012.03.100
23. Makihara, Y.; Umeda, K.; Shoji, F.; Kato, K.; Miyairi, Y.; *J. Alloys Compd.* **2008,** *455*,385. **DOI:** 10.1016/j.jallcom.2007.01.109
24. Orimo, S.; Fujii, H.; Horie, S.; *J. Alloys Compd.***1995,** *231*, 766. **DOI:** 10.1016/0925-8388(95)01715-1
25. Wang, P.; Wang, A.; Zhang, H.; Ding, B.; Hu, Z.; *J. Alloys Compd.* **2000,** *297*, 240. **DOI:** 10.1016/S0925-8388(99)00590-3
26. Yang, J.; Ciureanu, M.; Roberge, R.; *Mater. Lett.* **2000,** *43*, 234. **DOI:** 10.1016/S0167-577X(99)00265-7
27. Fernández, J.F.; Bodega, J.; Sánchez, C.R.; *J. Alloys Compd.* **2003,** *356-357*, 343. **DOI:** 10.1016/S0925-8388(02)01226-4
28. Agarwal, S.; Aurora, A.; Jain, A.; Jain, I.P.; Montone, A.; *Int. J. Hydrogen Energy* **2009,** *34*, 9157. **DOI:** 10.1016/j.ijhydene.2009.09.034
29. Agarwal, S.; Aurora, A.; Jain A.; Montone, A.; *J. Nanopart. Res.* **2011,** *13*, 5719. **DOI:** 10.1007/s11051-010-0203-0
30. Agarwal, S.; Jain, A.; Jain, P.; Jangir, M; Jain, I.P.; *J. Phys. Chem. C* **2013**, *117*, 11953. **DOI:** 10.1021/jp402085s
31. Jain, A.; Agarwal, S.; Jain, P.; Gislon, P.; Prosini, P. P.; Jain, I.P.; *Int. J. Hydrogen Energy* **2012**, *37*, 3665. **DOI:** 10.1016/j.ijhydene.2011.04.042
32. Sinha, V.K.; Yu, G.Y.; Wallace, W.E.; *J. Less-Common Met.* **1985,** *106*, 67. **DOI:** 10.1016/0022-5088(85)90367-4
33. Jain, A.; Agarwal, S.; Vyas, D.; Jain, P.; Jain, I.P.; *Int. J. Hydrogen Energy* **2010**, *35*, 9910. **DOI:** 10.1016/j.ijhydene.2011.04.042
34. Okamoto, H.; *J. Phase Equilib. Diffus.* **2007,** *28,* 305. **DOI:** 10.1007/s11669-007-9060-7; (b) Okamoto, H.; *J. Phase Equilib.* **2000,** *21*, 209. **DOI:** 10.1361/105497100770340336; (c) Okamoto, H.; *J. Phase Equilib. Diffus.* **2008,** *29*, 208. **DOI:** 10.1007/s11669-008-9272-5
35. Jain, A.; Jain, R.K.; Agarwal, G.; Jain, I.P.; *J. Alloys Compd.***2007,** *438*, 106. **DOI:** 10.1016/j.jallcom.2006.08.007; (b) Jain, A.; Jain, R.K.; Sharma, R.K.; Kumar, M.; Jain, I.P.; *J. Mag. Mag. Mater.*, **2007,** *318,* 44. **DOI:** 10.1361/105497100770340336 ; (c) Jain, A.; Jain, R.K.; Agarwal, S.; Sharma, R.K.; Kulshrestha, S.K.; Jain, I.P.; *J. Alloys Compd.* **2008,** *454,* 31. **DOI:** 10.1016/j.jallcom.2006.12.080
36. Zeng, K.; Klassen, T.; Oelerich, W.; Bormann, R.; *Int. J. Hydrogen Energy* **1999**, *24*, 989. **DOI:** 10.1016/S0360-3199(98)00132-3
37. Huot, J.; Liang, G.; Schulz, R.; *Appl. Phys. A: Mater. Sci. Process.* **2001**, *72*, 187. **DOI:** 10.1007/s003390100772
38. (a) Drašner, A.; Blažina, Ž.; *J. Less-Common Met.* **1990,** *163*, 151. **DOI:** 10.1016/0022-5088(90)90094-Z; (b) Qian, S.; Northwood, D.O.; *J. Less-Common Met.* **1989,** *147*, 149. **DOI:** 10.1016/0022-5088(89)90158-6; (c) Drašner, A.; Blažina, Ž.; *J. Less-Common Met.* **1991,** *175*, 103. **DOI:** 10.1016/0022-5088(91)90354-7; (d) Hirosawa, S.; Pourarian, F.; Sinha, V.K.; Wallace, W.E.; *J. Mag. Mag. Mater.*, **1983,** *38,* 159. **DOI:** 10.1016/0304-8853(83)90040-9

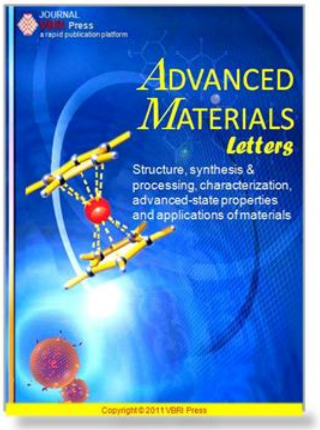
ADVANCED MATERIALS Letters
Structure, synthesis & processing, characterization, advanced-state properties and applications of materials
Copyright © 2011 VBRI Press